# A Large-Conductance Anion Channel of the Golgi Complex

Roger J. Thompson,*† Mark H. Nordeen,* Kathryn E. Howell,* and John H. Caldwell*†
Departments of *Cellular and Structural Biology and †Physiology and Biophysics, University of Colorado Health Sciences Center, Denver Colorado 80262 USA

ABSTRACT An acidic lumenal pH is vital for the proper posttranslational modifications and sorting of proteins and lipids from the Golgi complex. We characterized ion channels present in Golgi fractions that have been cleared of transiting proteins. A large conductance anion channel was observed in ~30% of successful channel incorporations into the planar lipid bilayer. The channel, GOLAC-2, has six levels (one closed and five open). The open states are each ~20% increments of the maximal, 325 pS conductance. The channel was ~6 times more selective for $Cl^-$ over $K^+$. Binomial analysis of percent occupancy for each conducting level supports the hypothesis of five independent conducting pathways. The conducting levels can coordinately gate because full openings and closings were often observed. Addition of 3 to 5 mM reduced glutathione to the *cis* chamber caused dose-dependent increases in single channel conductance, indicating that the channel may be regulated by the oxidation-reduction state of the cell. We propose that GOLAC-2 is a co-channel complex consisting of five identical pores that have a coordinated gating mechanism. GOALC-2 may function as a source of counter anions for the $H^+$-ATPase and may be involved in regulating charge balance and membrane potential of the Golgi complex.

## INTRODUCTION

The Golgi complex functions to modify and transport newly synthesized proteins and lipids and to sort these proteins and lipids as they exit the Golgi. Soluble and transmembrane proteins, as well as glycolipids and glycosphingolipids, transit through the Golgi, and the major posttranslational modifications to all these molecules are glycosylation and sulfation (Varki, 1998; van Meer, 2001). Central to the proper modification and sorting of proteins and lipids as they exit the Golgi is an acidic lumenal pH, which decreases from the *cis* (entry face) to the *trans* (exit face) Golgi (Anderson and Pathak, 1985). Measurements of Golgi lumenal pH have yielded values ranging from 5.95 (Demaurex et al., 1998) to 6.45 (Anderson and Pathak, 1985; Llopis et al., 1998), ~1 pH unit lower than the cytoplasm. Abolition of the acidic lumenal pH by $NH_4Cl$ results in improperly glycosylated and sorted proteins (Kelly, 1985). This is likely because many of the more than 200 nucleoside-sugar transporters and enzymes that are estimated to be resident in the Golgi complex function optimally under acidic conditions (Berger and Roth, 1997; Varki, 1998; Hirschberg et al., 1998).

Acidity of the Golgi lumen is maintained by an electrogenic $H^+$-ATPase (Glickman et al., 1983). The activity of this proton pump would cause a membrane potential to develop across the Golgi (Al-Awqati, 1995); however, measurements have suggested that there is no, or only a small intrinsic Golgi membrane potential (Llopis et al., 1998). A membrane potential would be detrimental for the proper function of this organelle because a well-known characteristic of $H^+$-ATPases is that $H^+$ pumping and ATP hydrolysis are slowed by the presence of a membrane potential (Glickman et al., 1983). Thus, accumulation of charge in the Golgi lumen would reduce the effectiveness of the pump and shift the pH beyond the optima of endogenous enzymes. It has been suggested that the Golgi is endowed with an endogenous mechanism for removing or buffering charge (Al-Awqati, 1995). Indeed, the first description of the proton pump of the Golgi demonstrated a parallel $Cl^-$ conductance (Glickman et al., 1983), and subsequent studies have demonstrated that $Cl^-$ contributes ~50% to the rate of Golgi acidification (Demaurex et al., 1998).

Candidates for the mediators of a Golgi $Cl^-$ conductance could be either anion channels or exchangers. The chloride intracellular ion channel family (CLIC) has seven known members, based on sequence homology to the p64 chloride channel of bovine kidney microsomes (Landry et al., 1993; Berryman and Bretscher, 2000). The CLIC channels have a broad intracellular distribution, and p64 (Landry et al., 1993), CLIC1 (Tulk et al., 2000), and CLIC4/p64H1 (Duncan et al., 1997) are thought to be functional chloride channels, based upon measurement of single-channel properties or $Cl^-$ efflux assays. Another possible chloride channel family is MCLC, which may be an anion channel or an activator of anion channels (Nagasawa et al., 2001). Several members of the voltage-gated chloride channel (ClC) family and the yeast homologue GEF1 (glycerol/ethanol Fe-requiring; Gaxiola et al., 1998) are thought to have specific intracellular distributions (for review, see Jentsch et al., 1999 ) and may provide a $Cl^-$ conductance for the Golgi.

Golgi ion channels are potential targets of regulatory pathways, such as phosphorylation or reduction-oxidation reactions. Redox regulation of ion channels has been described for several types of $Cl^-$, $Na^+$, and $K^+$ channels that

*Submitted December 28, 2001, and accepted for publication March 18, 2002.*

Address reprint requests to Dr. John H. Caldwell, Campus Box B-111, Department of Cellular and Structural Biology, University of Colorado Health Sciences Center, 4200 E. Ninth Avenue, Denver, CO 80262. Tel.: 303-315-6892; Fax: 303-315-4729; E-mail: john.caldwell@uchsc.edu.



0006-3495/02/07/278/12 $2.00

are endogenous to both the plasmalemma and organelles (for review, see Kourie, 1998). Redox molecules, such as glutathione and superoxide, rapidly and reversibly regulate ion channel function and may act as second messengers to regulate ion transport mechanisms, which can in turn affect intracellular $Ca^{2+}$ and membrane excitability. Recent results for the CLIC channels have focused attention on redox pathways. It has been suggested that the CLIC family of $Cl^-$ channels share homology with glutathione-S-transferase proteins (Dulhunty et al., 2001), and a recently published crystal structure of the soluble CLIC 1 protein confirms the presence of a glutathione binding site, suggesting that these intracellular anion channels may be subject to regulation by glutathione (Harrop et al., 2001).

Work in our laboratory has recently described an endogenous Golgi anion channel, GOLAC (that we now rename GOLAC-1), which has multiple conducting states and a maximal conductance of ~130 pS (Nordeen et al., 2000). Here we describe a large-conductance anion channel, which we call GOLAC-2, that is endogenous to the Golgi complex. GOLAC-2 exhibits five open states, discriminates poorly between different halide ions, shows no pH dependence in the physiological range, and increases its conductance in response to physiological concentrations of the reduced form of glutathione (GSH). GOLAC-2 differs significantly from the previously characterized GOLAC-1 channel and is a new member of a Golgi anion channel family.

## MATERIALS AND METHODS

### Chemicals and solutions

Lipids for the formation of planar bilayers were a mixture of POPE (1-palmitoyl-2-oleoyl-*sn*-glycero-3-phosphoethanolamine) and POPS (1-palmitoyl-2-oleoyl-*sn*-glycero-3-[phospho-L-serine]) at a ratio of 3:1 in decane and were obtained from Avanti Polar Lipids (Alabaster, AL). All other chemicals were from Sigma (St. Louis, MO). The standard recording solutions contained 150 mM KCl, 1.2 mM $CaCl_2$, 1 mM $MgCl_2$, 10 mM MOPS, 1 mM EGTA, adjusted to pH 7.0 with CsOH. For anion replacement experiments, equal activity of the test anion was substituted for $Cl^-$ on the *trans* side.

### Isolation of Golgi fraction enriched in endogenous proteins

Membrane fractions enriched in the Golgi complex (CHX SGF1) that were cleared of proteins in transit were prepared as previously described (Taylor et al., 1997). Briefly, Wistar rats were treated with cyclohexamide (50 mg/kg) for 4 h to inhibit protein synthesis and permit clearance of transiting proteins before livers were harvested. A typical preparation yielded 1.2 mg/mL of protein that was enriched 400- to 700-fold for Golgi markers and cleared of >99% of cargo proteins (Taylor et al., 1997). Five different preparations (6 to 12 rats each) were used for the experiments to characterize GOLAC-2.

### Electrophysiology

All recordings of Golgi ion channel activity were made using the planar lipid bilayer technique. Bilayers were formed across a 150- or 200-$\mu$m hole drilled into Delrin cuvettes (Warner Instruments, Waterbury, CT). To facilitate bilayer formation, the cuvette aperture was precoated for ~20 min with 0.5 to 1 $\mu$L of the lipid solution (defined above). Spontaneous bilayer formation was monitored as an increase in the capacitance to ~200 pF. Channels were allowed to spontaneously incorporate into the bilayer after addition of 6 to 20 $\mu$g protein from a Golgi fraction, which was added to the *cis* chamber. An osmotic gradient of 10 to 150 mM KCl (*trans* to *cis*) and a −50 mV holding potential (*trans* side was held at ground) with constant stirring of the *cis* chamber were used to aid in vesicle fusion. Isolated Golgi fractions retain the native orientation (i.e., cytoplasmic-face out; Perez and Hirschberg, 1987), suggesting that after successful Golgi membrane fusion with the lipid bilayer, the cytoplasmic and lumenal faces of the channel will be exposed to the *cis* and *trans* chambers, respectively.

Currents (I) are referred to as the flow of positive charge, and the *trans* chamber is defined as ground. Data were collected at 5 or 20 kHz under voltage-clamp and low-pass Bessel filtered at 1 kHz with an Axopatch 1B amplifier, Digidata 1380 analog to digital converter and pClamp (v. 8.0) software (all from Axon Instruments, Foster City, CA). Current-voltage (I-V) plots were determined for recordings of membrane potential from −100 mV to +100 mV (in 25-mV increments).

### Data analysis

All data were digitally Gaussian filtered at 500 Hz before analysis, except those used for mean-variance analysis (Patlak, 1993; Nordeen et al., 2000), which were not further filtered beyond the 1 kHz (−3 dB) cutoff frequency used during collection. Unitary current amplitudes for each conducting state at each holding potential were determined by fitting single Gaussian curves to amplitude histograms generated using the 50% threshold method by pClamp (Fetchan and Pstat) version 6.0.3. The user made initial estimates of single channel amplitudes. Events that were briefer than 2 ms were ignored during 50% threshold analysis to ensure that only full, stable current transitions were binned (256 total bins) in each amplitude level. Typically, GOLAC-2 had five open levels and one closed level. The presence of multiple states was confirmed by either "all-points" amplitude histograms generated by pClamp or by three-dimensional mean-variance (M-V) plots. M-V plots were generated using Levels, a program that was written and provided by Dr. Diego Restrepo (University of Colorado Health Sciences Center).

Mean dwell times for each subconducting state were determined with either pClamp 6 or Levels software. However, neither method was considered ideal because 1) the signal-to-noise ratio was often low, which leads to an underestimate of dwell times using the 50% threshold method (Colquhoun and Hawkes, 1995) and 2) dwell times were often very short, and these events are either improperly binned or ignored (Colquhoun and Hawkes, 1995; Patlak, 1993). However, restricting the analysis to recordings at ±100 mV improved the signal-to-noise ratio, and limiting the analysis to exclude events shorter than 2 ms allowed for a more accurate measure of dwell times. During analysis of dwell times, care was taken to select the regions of lowest variance for each amplitude level (i.e., the densest portion of the mean-variance plot for each amplitude level; see Fig. 2). Although these restrictions reduce the ability to detect rapid events, this method allowed us to be confident that dwell times corresponded only to each amplitude level. Mean open probability ($p_o$) was determined as the area under current amplitude histograms for each substate as generated by pClamp or as the volume under each amplitude level in the three-dimensional M-V plots that were generated by Levels. The two methods typically yielded similar results.

Binomial analysis of the average percent occupancy of each substate was used to determine if the distribution of substates could arise from five independently gating conducting pathways (Krouse et al., 1986; Morier

and Sauve, 1994). Observed occupancies ($p_o$) for each substate (L0-L5) of the channel were fit to a binomial equation of the form

$$p_{(o,n)} = [5!/(5 - n)!]p^n(1 - p)^{5-n} \quad (1)$$

in which $p_{(o,n)}$ is the observed occupancy for each substate, $n$, of five total states, and $p$ is that probability of finding any one level in the open state. Values of $p$ were determined by Sigma Plot (Jandel Scientific) to be the best fit for the $p_o$ data. Use of the binomial relationship assumed that there were $n$ identical channels or pores gating independently, and a good fit to Eq. 1 is considered to support this assumption.

Relative anion permeability ($P_x$) of GOLAC-2 was estimated for various test anions, $X$, relative to $Cl^-$ ($P_x/P_{Cl}$). $P_x/P_{Cl}$ was determined as $0.16 - 1.16e^{(Erev/-25.69)}$, in which $25.69 = RT/F$ and $E_{rev}$ is the reversal potential (i.e., zero current potential) measured upon replacement of $Cl^-$ with anion $X$ in the *trans* chamber. Calculations were based on the activities of the ions. The contribution of $K^+$ permeability ($P_K = 0.16P_{Cl}$; see below) to the total relative ionic permeability was incorporated in the calculation, and we have assumed that different anions do not alter the relative $K^+$ permeability of GOLAC-2. Plots of $P_x/P_{Cl}$ versus the Stokes diameter of each anion were used to estimate the pore size of the channel (Bormann et al., 1987). Corrections for liquid junction potentials that arise during exchange of solutions with different anion composition were made using the junction potential calculator software (written by Dr. Peter Barry, University of New South Wales, Australia) that is part of the pClamp 8.0 suite of programs.

## RESULTS

### Large conductance anion channels are present in endogenous Golgi membrane fractions

We have recently reported the presence of an anion channel, GOLAC-1, which is present in a highly enriched Golgi fraction (Nordeen et al., 2000). GOLAC-1 was approximately three times more selective for $Cl^-$ versus $K^+$ ions, had five (and sometimes six) conducting levels with a maximal conductance of ~130 pS. During the characterization of GOLAC-1, larger conductance anion channels were also frequently observed, and that channel is characterized here.

In 109 successful channel incorporations into artificial planar lipid bilayers, ~30% (35/109) were this single large conductance anion channel (GOLAC-2). The remaining successful channel incorporations were comprised of GOLAC-1, cation, smaller anion, or multiple channels of the same or mixed types. GOLAC-2 had a measured reversal potential ($E_{rev}$) of 38 ± 1 mV ($n = 15$) in asymmetrical KCl solutions (10 mM *trans* and 150 mM *cis*). For comparison, a purely $Cl^-$ selective channel would have had an $E_{rev}$ ~70 mV under these conditions, and $E_{rev}$ for GOLAC-1 was ~22 mV (Nordeen et al., 2000). With the Goldman-Hodgkin-Katz equation, GOLAC-2 was determined to be 6.1 times more selective for $Cl^-$ than $K^+$. Based on the markedly different relative $Cl^-$: $K^+$ selectivity ratio for GOLAC-1 and GOLAC-2, we were confident that GOLAC-2 did not consist of multiple GOLAC-1 channels that had inserted simultaneously into the bilayer. This was confirmed by comparing unitary channel conductance and relative anion permeability (see below).

Fig. 1 *A* shows typical recordings from a GOLAC-2 channel in symmetrical 150 mM KCl solutions at holding potentials between ±100 mV as indicated. An all-points current-amplitude histogram for the channel in Fig. 1 *A* ($V_m = -100$ mV) is shown in Fig. 1 *Bi*. This analysis routinely revealed the presence of five open states (L1-L5) and one closed state (L0) that were separated by approximately equal current increments, suggesting that the open state of GOLAC-2 is comprised of at least five conducting levels (see below for additional analysis that rules out the possibility that five independent, identical channels simultaneously incorporated into the bilayer). This was confirmed during generation of an "events list" in which an idealized trace of the current record is generated by pClamp. Fig. 1 *Bii* is the histogram of the events list generated from the idealized trace of the record in Fig. 1 *Bi*, and clearly shows five equally spaced open levels (L1-L5). Current-voltage (I-V) plots were linear between ±50 mV and showed inward rectification at potentials more negative than −75 mV. This is illustrated in the I-V plot of Fig. 1 *C*, which is a composite for nine separate GOLAC-2 single channel recordings. The inward rectification of GOLAC-2 was approximately the same for each substate (a twofold increase in conductance at −100 mV).

The slope conductance of the five open states of GOLAC-2 was determined over the linear range of the I-V relationship (±50 mV). Conductance increased by equal increments of ~65 pS and reached a maximum of 328 ± 20 pS ($n = 15$; mean ± SE) for L5. The open subconducting levels, L1-L4, were determined to be 72 ± 3 (L1), 133 ± 5 (L2), 202 ± 8 (L3), and 262 ± 10 pS (L4) for these 15 channels, which correspond to ~22%, 41%, 62%, and 80% of the fully open level (L5), respectively. Smaller conductance levels of ~20 pS (the conductance of GOLAC-1 substates) were rarely found to be superimposed on the GOLAC-2 recordings. If present, these smaller conductance levels could be attributed to contamination of the record by GOLAC-1 channels, and these data were excluded from further analysis.

### Substate behavior and coordinated gating of GOLAC-2

The presence of multiple open states in Golgi anion channels was observed in the "all-points" amplitude histograms generated at a holding potential of −100 mV (e.g., Fig. 1 *Bi*). Multiple current levels in a recording could arise from several channels incorporating into the bilayer simultaneously, by a single pore with multiple conducting states, or by a single multipore complex. Single GOLAC-2 channels were consistently observed to have five open levels. In two cases where anion channels with only one to four current levels were observed, they were clearly distinguishable from the GOLAC channels based on $E_{rev}$ measurements and conductance. Recordings that had greater than six current

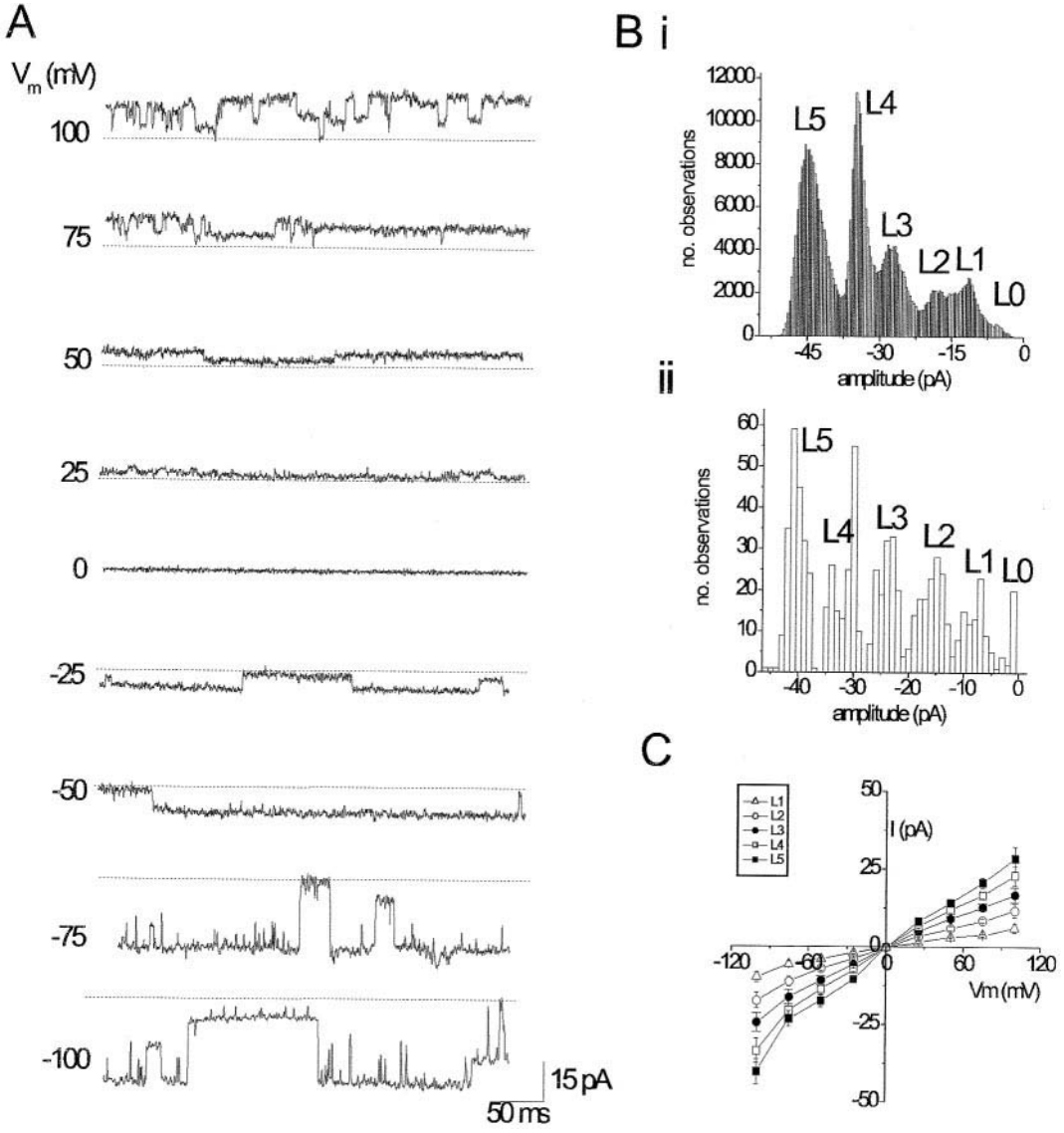


FIGURE 1 Voltage-dependence of channel conductance states in symmetrical 150 mM KCl. (*A*) Representative 500-ms recordings of single-channel activity at different membrane potentials ($V_m$) as indicated to the left of each trace. The dotted line indicates the closed state. (*B*) An all-points amplitude histogram (*i*) and an "events-list" histogram (*ii*) for the channel in *A* at a $V_m$ of −100 mV showing the closed (L0) and five open (L1-L5) levels. (*C*) Average current-voltage relationship of each open level ($n = 9$). Note the inward rectification at potentials more negative than −75 mV.

levels could be attributed to the incorporation of multiple channels in the bilayer because full openings or closings were not seen; these records were excluded from further analysis.

Substate occupancy of GOLAC-2 channels was voltage-dependent (Fig. 2). Using M-V analysis, with a window width of 21 or 51 data points, we constructed M-V plots to estimate dwell times and open probabilities at +100 and −100 mV (Fig. 2, *A* and *B*). In the three-dimensional M-V plots of Fig. 2, *A* and *B*, each peak (e.g., red and yellow regions of density) represents a single, stable current level (i.e., region of low variance) that is analogous to the peaks in the "all-points" histogram of Fig. 1 *Bi*. Note that both the all-points (Fig. 1 *Bi*) and M-V (Fig. 2 *A*) analyses clearly show the presence of five open states (L1-L5) and one closed state (L0) at −100 mV. However, at +100 mV the channel entered a bursting mode that consisted of rapid transitions (Fig. 2 *D*, current traces), which made analysis of dwell times difficult to resolve, and the time constants obtained were similar to the sampling frequency (100–200 μs) or minimal detectable event duration (2 ms), which was determined as twice the sum of the rise times of the 1 kHz (~330 μs) and 500 kHz (~660 μs) filters (Colquhoun and Sigworth, 1995). Examination of the M-V plot in Fig. 2 *B* shows an overlap of the amplitude peaks (compare with the M-V histogram in Fig. 2 *A*), which is indicative of short dwell times and/or an unstable baseline (Patlak, 1993).

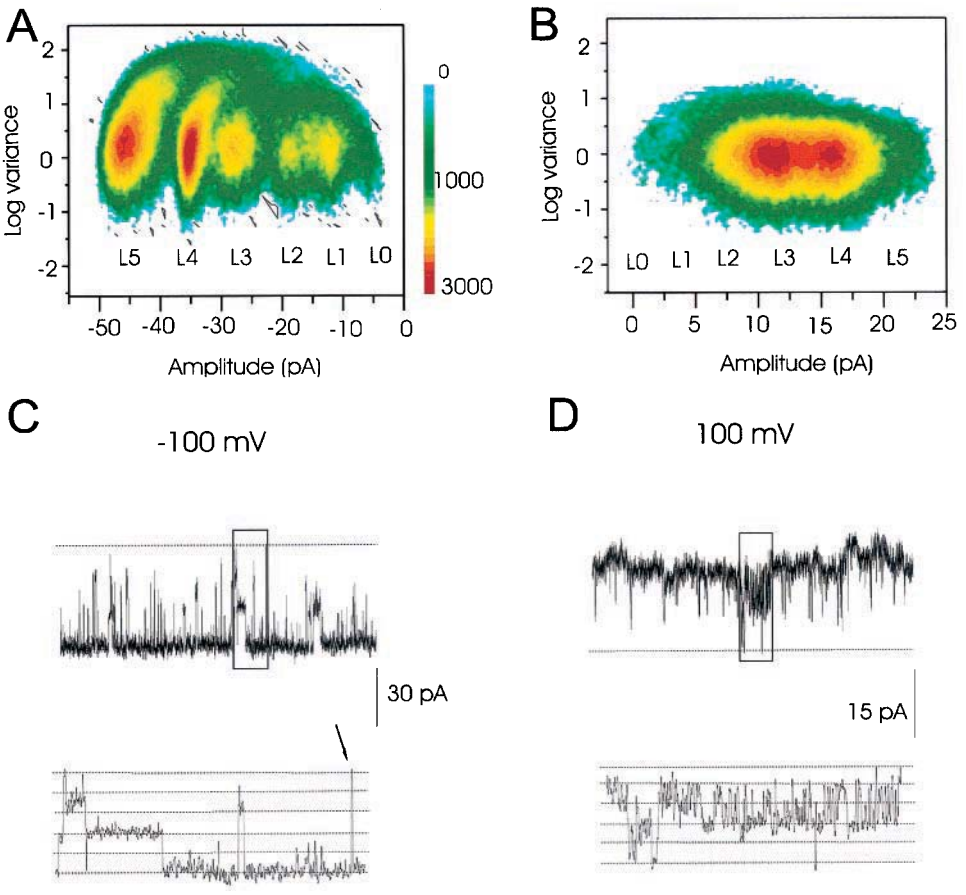


FIGURE 2 Voltage-dependence of substate behavior. (*A*) Mean variance plot calculated at a window width of 21 data points for the recording in *C*. Each amplitude level (L0-L5) is indicated and clearly distinguishable. (*B*) Mean-variance plot for the trace in *D*, calculated at a window width of 21 data points. Note that transitions between substate levels (L0-L5) were rapid, which resulted in poor resolution of individual amplitude levels in the mean-variance histogram. The colored scale bar represents counts per amplitude bin. Inward rectification is evident from the difference in current amplitudes at −100 mV compared with +100 mV. (*C*) Representative 5-s traces (*upper panel*) of GOLAC-2 channel activity recorded at $V_m = -100$ mV. The lower panel corresponds to a 500-ms portion of the recording as indicated by the box in the upper panel. Five open levels are clearly visible and marked by dotted lines. Note the full closing (*arrow*), followed rapidly by a full opening, of the channel, indicating a coordinated gating mechanism. (*D*) Representative 5-s trace (*upper panel*) of the same channel shown in *C* at $V_m = +100$ mV. The boxed region is a 500-ms portion of the trace that is expanded in the lower panel.

At −100 mV, substate transitions to open levels were more stable, and M-V plots could be used to estimate dwell times and open probability (Figs. 2 *C* and 3). In most cases, time constants for each open level (at −100 mV), were fit by a single exponential (Fig. 3 *A*), and rarely (<10% of records) a faster component (~5 ms) was observed. The dwell time distribution of Fig. 3 *A* is for L4 of a single GOLAC-2 channel and was fit by a single exponential with a time constant of 108 ms ($R^2 = 0.99$). Mean dwell times for each of the open levels and the closed state were determined as in Fig. 3 *A* and are plotted in Fig. 3 *B*. The average dwell time at any one level was ~100 ms with the exception of brief transitions to the fully closed state, which were sometimes poorly resolved. GOLAC-2 was found to be open ~95% of the time, regardless of membrane potential (Fig. 3 *C*). Individual substates appeared to be randomly gated, and transitions between any given open level and the closed state were observed, suggesting that the substates gated independently of each other except during the coordinated entry and exit from L0 (see below). Independent gating was observed at all membrane potentials.

To address the possibility that the substates of GOLAC-2 gate independently, we used binomial analysis to determine if the observed occupancies of each level were random (Morier and Sauve, 1994). Observed occupancy ($P_o$) was determined as the proportion of time the channel spent in a given state. Predicted occupancy ($P_{pred}$) was estimated from the binomial distribution for the $p$ value that best fit the data (see Materials and Methods). Fit of the $p_o$, at −100 mV, to the binomial equation was best with $p = 0.91$, and the results of a fit for three GOLAC-2 channels are shown in Fig. 4. A plot of $p_o$ versus $P_{pred}$ (inset of Fig. 4) was well fit with a straight line of slope = 1.05 ± .04 ($R^2 = 0.99$), suggesting that each subconducting level of GOLAC-2 was gating independently. $p_o$ and $P_{pred}$ also agreed at other membrane potentials.

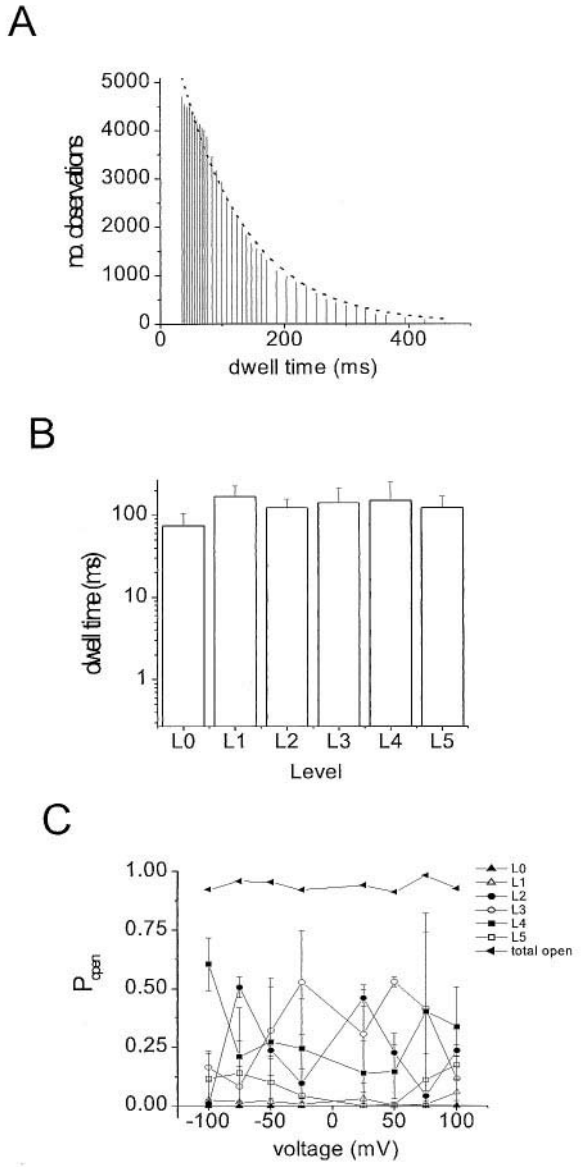


FIGURE 3 Kinetic behavior of GOLAC-2 at −100 mV. (*A*) Exemplar dwell time distribution for L4 of a GOLAC-2 channel and fit with a single exponential of time constant = 108 ms (*dotted line*). (*B*) Mean dwell time of each level (L0-L5) for six GOLAC-2 channels (except for the closed state where $n = 4$). Bars are the average dwell time at each level. Note the logarithmic ordinate. (*C*) Open probability of each level as a function of membrane potential. The channel was rarely closed at any potential (95% "total open").

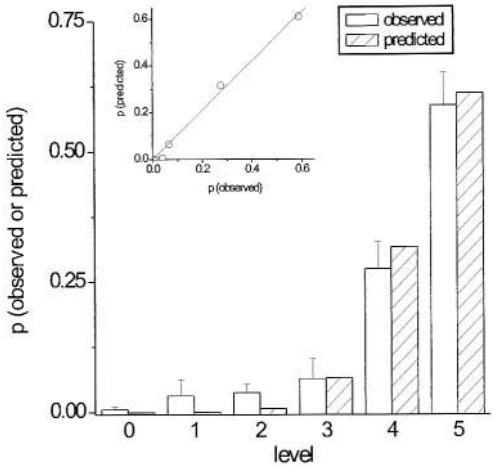


FIGURE 4 Binomial analysis of observed occupancy for each substate. Observed occupancy (i.e., percent time at each level) was best fit to a binomial distribution with $p = 0.91$ ($p$ = probability of any state being open). The inset is a test for goodness of fit of the observed occupancy to that predicted by the binomial equation at $p = 0.91$. Calculations are based on three GOLAC-2 channels at a holding potential of −100 mV and are consistent with substate transitions occurring independently.

The goodness of fit of $p_o$ with the binomial equation is consistent with the presence of at least five independent conducting pathways in the GOLAC-2 channel, but this could arise from five separate, identical channels in the bilayer. Full closings and openings of GOLAC-2 within a single sampling interval were frequently observed (see Fig. 2 *C*, arrow), which argues against the presence of five completely independent and separate channels. If five channels had simultaneously incorporated into the bilayer instead of a single channel with multiple open levels, these rapid full transitions would require simultaneous closing (or opening) of all the channels. The probability of observing a full transition during a typical 20-s recording period (sampling interval was 100 $\mu$s) can be estimated as the product of the probability of each substate closing times the number of sampling intervals. For each substate, the closing probability was estimated to be $10^{-2}$ (L1) to $10^{-3}$ (L2-L5) from the equation [1 − exp(−sample interval/mean open time)] (Krouse et al., 1986). Thus, the probability that five channels with the dwell times determined for each of the conducting states of GOLAC-2 (Fig. 3 *B*) opening or closing simultaneously was estimated to be $\sim 10^{-9}$ for each 20-s recording episode. At least one full closing (and often three to five) was typically observed in any given 20-s recording interval. This strongly suggests that the five open levels of GOLAC-2 can be coordinately gated by a common mechanism and indicate a single functional complex.

## Anion selectivity

$Cl^-$ on the *trans* (lumenal equivalent) side of the bilayer was replaced by exchanging the solution with 8 to 10 volumes of one containing $K^+$ salts of test anions (X) to investigate the ionic selectivity of GOLAC-2. Two properties can be derived from these experiments, anion permeability and anion conductance relative to $Cl^-$. Changes in relative anion permeability ($P_x/P_{Cl}$) are indicated by a shift in the reversal potential (abscissa intercept) upon replacement of $Cl^-$ in the *trans* chamber with an equal activity of the exchange anion. A shift of reversal potential in the

positive direction indicates that X is less permeant than $Cl^-$. A decrease in single channel conductance is indicated by a decrease in the slope of the I-V relationship, relative to that in symmetrical KCl. Fig. 5 *A* shows I-V plots for four GOLAC-2 channels after exchange of the 150 mM KCl solution in the *trans* chamber with a 150 mM solution containing the halide anion ($K^+$ salt). For GOLAC-2, the halide anion permeability sequence (relative to $Cl^-$) was $I^-$ (1.8) > $Br^-$ (1.1) > $Cl^-$ (1.0) > $F^-$ (0.43), which corresponds to Eisenman sequence 1 of the seven predicted anion permeability sequences (Wright and Diamond, 1977). Fig. 5 *B* is a plot of $P_X/P_{Cl}$, for all monovalent anions tested, versus the Stokes diameter of each anion. In general, relative anion permeability was a function of the ion's energy of hydration, such that anions that bind water more tightly (i.e., $F^-$) were less permeant. Gluconate, with a Stokes diameter of ~6.2 Å, was impermeant for all open levels, suggesting that the pore size of GOLAC-2 conducting states is less than 6.2 Å (similar to the predicted size of GOLAC-1). Additionally, all of the open levels had identical shifts in $E_{rev}$ during these anion replacement experiments. Taken together, these data suggest that the open levels of GOLAC-2 are comprised of the same pore-forming protein(s).

Changes in single channel conductance upon anion exchange, measured as the slope of each line in Fig. 5 *A*, showed a strong dependence on the Stokes diameter (Fig. 5 *C*). Some anions that have larger diameters than $Cl^-$ (e.g., $SCN^-$) were found to have decreased conductance relative to $Cl^-$, despite having increased relative permeability. This apparent contradiction has been observed for a variety of channels and reflects the fact that relative permeability (obtained by changes in reversal potential) is a measure of the intrinsic permeability of the pore, whereas conductance is a measure of the flux (Dawson, 1996; Hille, 2001). This type of channel behavior is indicative of ion binding in the pore and together with the permeability to both anions and cations, suggests a multiion pore. Anions that have stronger binding to sites in the pore will have a lower conductance but higher permeability. Anion exchange showed similar conductance changes for each of the open levels (data not shown). Sulfate, a divalent anion, was permeant but had no measurable conductance. Replacement of $Cl^-$ in the *trans* chamber with 75 mM $K_2SO_4^{2-}$ shifted the reversal potential to 24 ± 2 mV ($n$ = 2) ($P_{sulfate}$:$P_{chloride}$ = 0.2), and no conductance was measurable in either the inward or outward directions (data not shown). The relative anion permeability of $SO_4^{2-}$ to $Cl^-$ and the loss of conductance suggest that divalent anions bind within the pore and are poorly permeant.

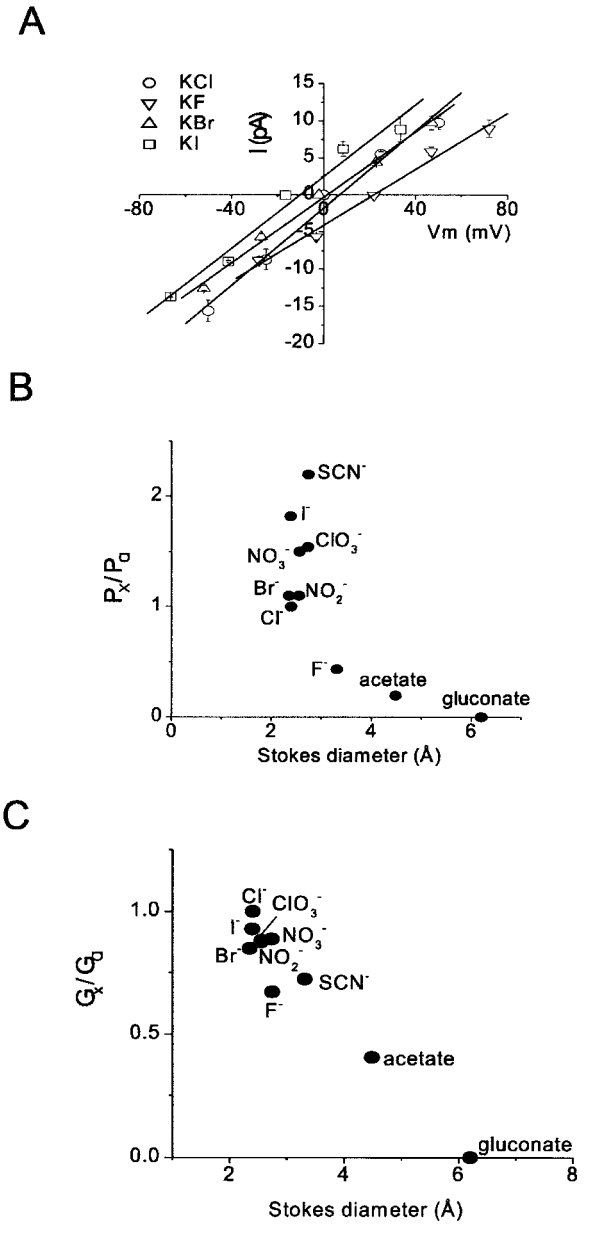


FIGURE 5 Anion selectivity of GOLAC-2. (*A*) Current-voltage relationships for four channels during replacement of KCl in the *trans* chamber by various $K^+$ salts, as indicated. A shift in reversal potential to the left indicates a more permeant anion. Slopes are indicated by the straight lines, which were calculated by least-squares linear regression of the data between ±50 mV. A decrease in slope indicates that the test anion has a reduced conductance compared with $Cl^-$. (*B*) Plot of relative anion permeability versus anion size. (*C*) Plot of relative anion conductance versus anion size. Note the differences in rank order of relative permeability and relative conductance for each anion (compare *B* with *C*).

## Block of GOLAC-2

The ability of two anion channel blockers, DIDS (4,4′-Diisothiocyanatostilbene-2,2′-disulfonic acid disodium salt) and IAA-94 (Indanyloxyacetic acid 94), to inhibit single channel currents through GOLAC-2 was tested. DIDS is a stilbene derivative that has a divalent negative charge and is a nonspecific inhibitor of anion channels. IAA-94 is a nonselective anion channel blocker that inhibits CLIC1 with an $EC_{50}$ of ~ 8 $\mu$M and was used to isolate the p64 and

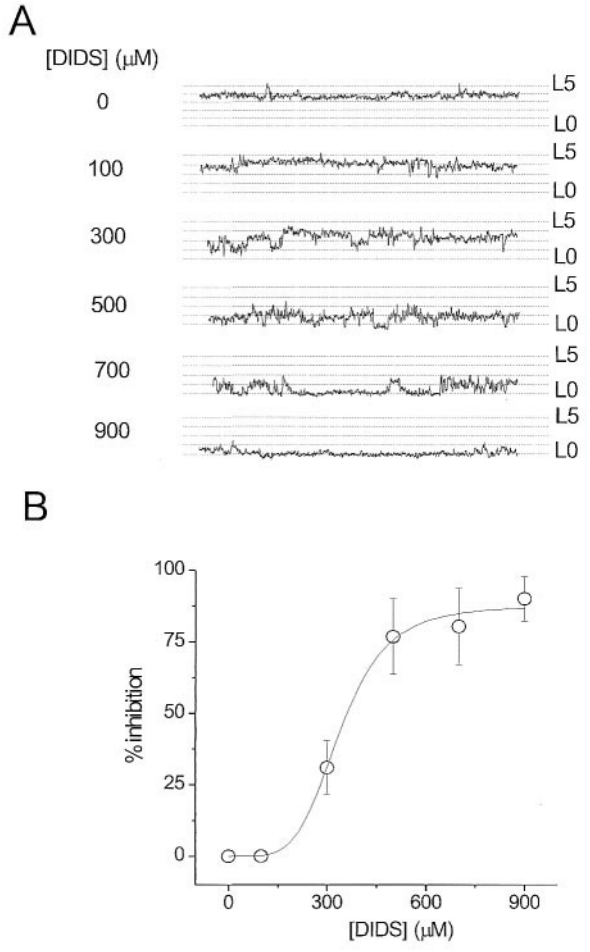


FIGURE 6 GOLAC-2 is blocked by DIDS in a concentration-dependent manner. (*A*) Exemplar recordings of a GOLAC-2 channel (at +50 mV) with increasing concentrations of DIDS (as indicated) added to the *trans* chamber. (*B*) Mean concentration-response curve for three GOLAC-2 channels. The ordinate represents percent inhibition of total channel open probability upon addition of increasing concentrations of DIDS relative to the control value. The solid line is fit of the data with the Hill equation, $y = V_{max}\,(x^n/(EC_{50}{}^n + x^n))$, in which $y$ is inhibition at DIDS concentration, $x$. $V_{max}$ is the maximal inhibition, $EC_{50}$ is the concentration to achieve 50% of $V_{max}$, and $n$ is the Hill coefficient.

CLIC1 channels (Landry et al., 1993; Tulk et al., 2000). Addition of DIDS to either the *trans* or *cis* side of the bilayer caused a concentration-dependent inhibition of GOLAC-2, characterized by progressive increased occupancy of the lower conductance levels (Fig. 6 *A*). Fit of the concentration-response curve in Fig. 6 *B* with Hill's equation (solid line) showed that addition of DIDS to the *trans* chamber inhibited all of the current levels of GOLAC-2, with an $EC_{50}$ of 229 ± 23 μM ($n$ = 3, Hill coefficient = 1.8 ± 0.2, $R^2$ = 0.99). Similar results were obtained when DIDS was added to the *cis* chamber (not shown). The effect of DIDS was not reversible, suggesting that it binds tightly to, or irreversibly alters the channel. In contrast to DIDS, addition of IAA-94 to either the *trans* or *cis* chambers, at concentrations ranging from 5 to 500 μM did not affect GOLAC-2 activity ($n$ = 4; data not shown).

### Physiological regulation of GOLAC-2

One proposed physiological function for the Golgi anion channels is to provide counter anions for the $H^+$-ATPase that maintains the acidic lumen of the Golgi complex. GOLAC-1, the first Golgi anion channel described, increased conductance during acidification, but not alkalinization, of the *trans* chamber (Nordeen et al., 2000). To determine if GOLAC-2 is pH sensitive, we tested the effects of changing the pH of the *trans* chamber on single channel properties. The I-V plots of Fig. 7 *A* were determined as the mean current for four GOLAC-2 channels exposed to the pH levels indicated. The conductance (the slope of a linear regression to the data between ±50 mV) was determined for each test pH. Acidification of the *trans* (lumenal) side of the channel moderately increased the single channel conductance of GOLAC-2 at pH values less than 5.2 (Fig. 7 *B*). However, no significant modification of single channel properties within the physiological range of pH (6.0–7.2) was observed. Note that similar changes in channel conductance upon acidification of the *trans* chamber were seen for each of the open levels. This further supports the hypothesis that GOLAC-2 is comprised of five identical pore-forming protein(s).

Anion channels of the CLIC family have structural homology to the glutathione-S-transferase super family and can bind glutathione (Dulhunty et al., 2001; Harrop et al., 2001). Additionally, ion channels from several families are sensitive to redox modulation (Kourie, 1998). The ability of the reduced form of GSH to modulate the single channel properties of GOLAC-2 was tested. Addition of GSH to the *cis* chamber, at concentrations similar to those found in the cytoplasm (1–5 mM) increased the conductance of all open levels, but did not affect dwell times or $P_{open}$. Exemplar traces (at $V_m$ = −50 mV) with GSH concentrations of 1.5 and 5 mM are shown in Fig. 8 *A*. Note that the unitary current amplitudes increased with higher concentrations of GSH; this is further illustrated in the histograms of Fig. 8, *C* (control) and *D* (5 mM GSH), which were derived from the idealized events lists of the traces in Fig. 8 *A*. Fig. 8 *B* summarizes the conductance change induced by 1.5 and 5 mM GSH for substate L3.

## DISCUSSION

Anion channels with multiple conducting states have been described in the plasma membrane (Krouse et al., 1986), endoplasmic reticulum (Clark et al., 1997), sarcoplasmic reticulum (Rousseau, 1989; Kourie et al., 1996), and Golgi complex (Nordeen et al., 2000), where they are thought to play roles in maintaining acidification and osmotic balance

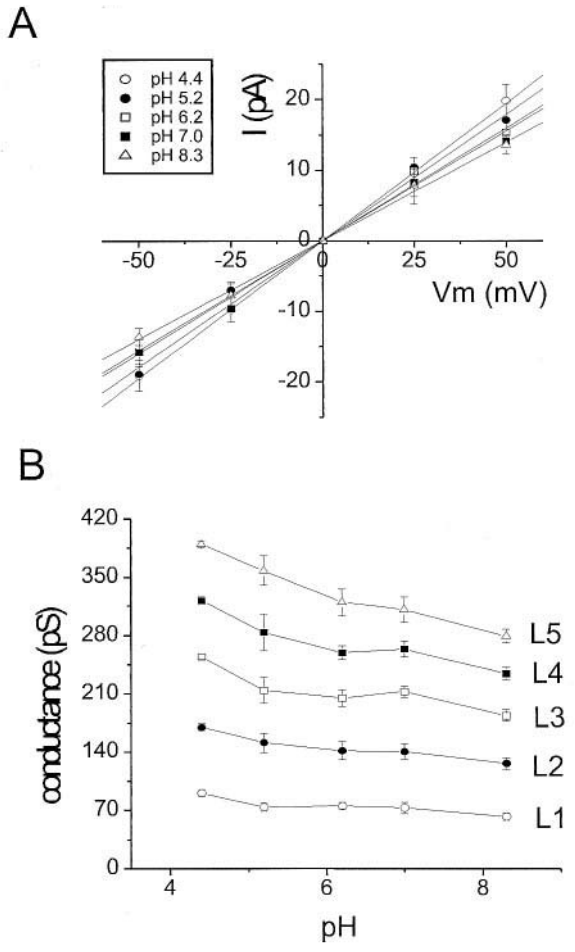


FIGURE 7 Effect of pH on GOLAC-2 anion channels. (*A*) Current-voltage plot for L4 at different pH in the *trans* chamber. Each point is the mean of four channels. (*B*) Conductance for each of the open levels increased when the *trans* pH was decreased below 5.2. Points are a mean of four GOLAC-2 channels. Note that there is no difference in conductance between pH 7.0 and 6.2.

(Al-Awqati, 1995). Here we describe a novel anion channel that is present in an enriched Golgi fraction that was reconstituted into planar lipid bilayers. This technique has been used successfully to record and characterize single channel activity of an intermediate conductance Golgi anion channel, GOLAC-1 (Nordeen et al., 2000). How certain can one be that these channels actually reside in the Golgi? Although all our enrichment data and morphological characterization indicate that these channels reside in the Golgi, one of the inherent difficulties of planar lipid bilayer recordings from subcellular fractions is that the fractions are never pure. Thus, there is always the possibility that the channels come from another organelle. Confirmation of the channel localization to the Golgi awaits the molecular identification and visualization of its subcellular distribution with epitope tags or immunolocalization.

Comparison of the biophysical properties of GOLAC-1 and GOLAC-2 support classification as different channels, but we consider them to be members of the same anion channel family for the following reasons. Both Golgi anion channels exhibited five predominant conducting levels (a sixth level was infrequently observed for each channel). The Golgi anion channels displayed equally spaced subconductance levels of ~20% of the fully open level. Although GOLAC-2 was much more selective for anions over cations than GOLAC-1, both channels had the lyotropic halide anion selectivity sequence (I>Br>Cl>F). Both showed similar pH-dependent changes in conductance, but for GOLAC-2 there was little change in the physiological range of pH. Both channels were sensitive to block by DIDS. Both channels were open over 95% of the time. Taken together, the similarities in channel properties, but marked differences in conductance and in anion/cation selectivity suggest that GOLAC-1 and GOLAC-2 are distinct members of an endogenous anion channel family of the Golgi complex.

An anion channel similar to GOLAC-2 with multiple, equal sized 60- to 70-pS substates has been described in pulmonary alveolar epithelial cell plasma membranes (Krouse et al., 1986). Some Golgi-resident proteins, such as TGN-38, shuttle between the plasma membrane and the *trans*-Golgi (Ladinsky and Howell, 1992; Bos et al., 1993). Thus, during membrane transport GOLACs may reside in membranes other than the Golgi. This might explain the presence of a channel very similar to GOLAC-2 in the plasma membrane of epithelial cells (Krouse et al., 1986).

To date, four families of anion channels have been described. They are the ClC family (voltage-dependent $Cl^-$ channels), the CLIC family ($Cl^-$ intracellular channels), the ABC family (ATP-binding cassette), and the ligand-gated anion channel family. Assignment of the Golgi anion channels to one of the known families of chloride channels is not possible at this time and will have to await identification of GOLAC-1 and GOLAC-2 at the molecular level. Some comparisons with the voltage-dependent chloride channel (ClC) family are notable: ClC-0, which was cloned from *Torpedo* electroplax, is an outward rectified, double-barreled channel comprised of two functional channel subunits that can gate independently or together (Jentsch et al., 1999; Mindell et al., 2001; Weinreich and Jentsch, 2001). Binomial analysis of substate gating and the frequency of full channel openings and closings support the possibility that GOLAC-2 is a co-channel complex with five independent pores that can be regulated by a coordinated gate, similar to the double-barreled motif of the ClC channels. However, GOLAC-1 and GOLAC-2 have either no voltage-dependence (GOLAC-1) or only moderate voltage-dependence (GOLAC-2), larger single channel conductance, and markedly different anion selectivity sequences than the ClC family of anion channels (see Jentsch et al., 1999). For these reasons, classification of the Golgi anion channels in the ClC family seems unlikely.

Another possibility is that Golgi anion channels are members of the chloride intracellular channel (CLIC) family. Of

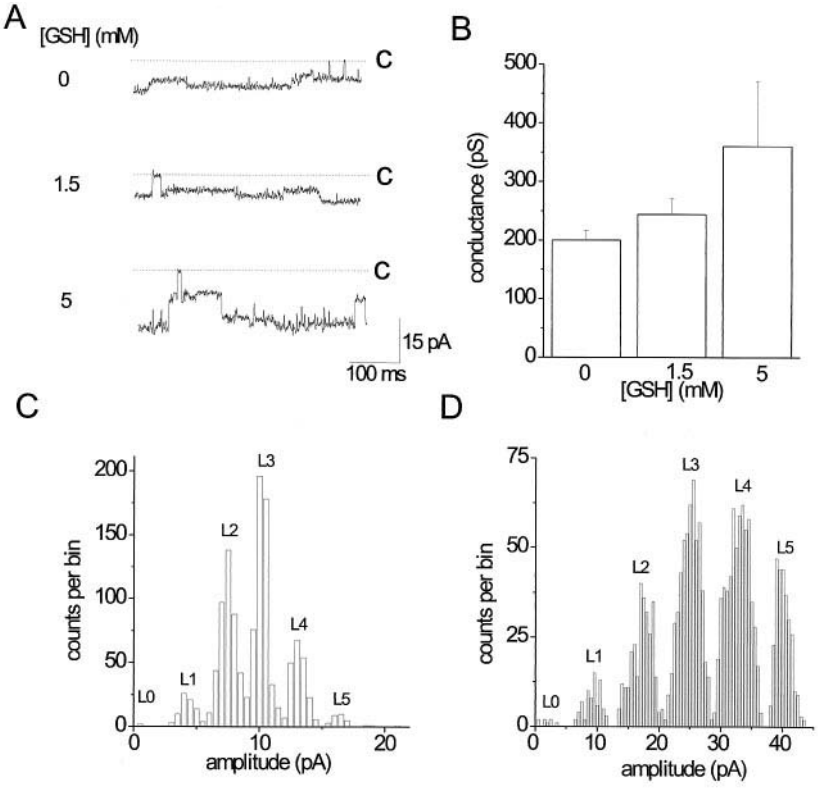


FIGURE 8 Reduced GSH increases conductance of GOLAC-2. (*A*) Exemplar traces from a GOLAC-2 channel at a membrane potential of −50 mV in the presence of increasing concentrations of GSH. (*B*) GSH increased conductance of L3 ($n = 3$) in a concentration-dependent manner. Similar results were seen for all of the open levels, L1-L5. (*C*) Amplitude histogram generated from the idealized trace of the record in *A*, showing the current levels of a GOLAC-2 channel (at −50 mV) under control conditions. (*D*) Amplitude histogram from the same channel as shown in *C* in the presence of 5 mM GSH in the *cis* chamber. Note that there is an equal shift of all amplitude levels.

the seven known CLIC channel homologues, only p64 (Landry et al., 1993), CLIC-1 (Tulk et al., 2000), and a rat homologue of CLIC4 (Duncan et al., 1997) are putative channels based on single channel recordings in planar lipid bilayers. The properties of the CLICs that have been expressed are different from those of the GOLACs. MCLC (mid-1-related chloride channel) is possibly another intracellular chloride channel family expressed in ER, Golgi, and nuclear membranes (Nagasawa et al., 2001). The single channel properties of MCLC were not characterized in detail, but it exhibited a 70-pS conductance in symmetrical 100 mM KCl. MCLC was not blocked by DIDS, and the existence of substates was not noted in the study. Thus, the single channel properties (i.e., voltage-dependence, anion selectivity, and IAA-94 sensitivity) of the previously described CLIC channels and MCLC are different enough from GOLAC-1 and GOLAC-2 to exclude identification of Golgi anion channels as p64, CLIC-1, or MCLC. The crystal structure of the soluble form of CLIC-1 indicates that this channel can bind and may be regulated by GSH (Harrop et al., 2001; see also Dulhunty et al., 2001), and GOLAC-2 conductance was augmented by GSH added to the *cis* chamber. The increase of GOLAC-2 conductance by GSH reported here raises the possibility that the Golgi anion channels are heretofore-uncharacterized members of the CLIC family of chloride channels. Of course, it is also possible the GOLAC-1 and GOLAC-2 belong to a novel ion channel family.

## Channel structure and possible physiological functions

The presence of five, equally spaced, open levels in GOLAC-2 could arise from different conducting conformations of a single pore, for example, one that has fivefold symmetry (Fig. 9 *A*) or from a multibarreled, co-channel complex (Fig. 9 *B*). The GABA and glycine ligand-gated anion channels are examples of the first possibility; both have a single pore, based on structural similarities to nicotinic acetylcholine receptors, and have multiple, unequal conductance levels (Bormann et al., 1987). An example of the

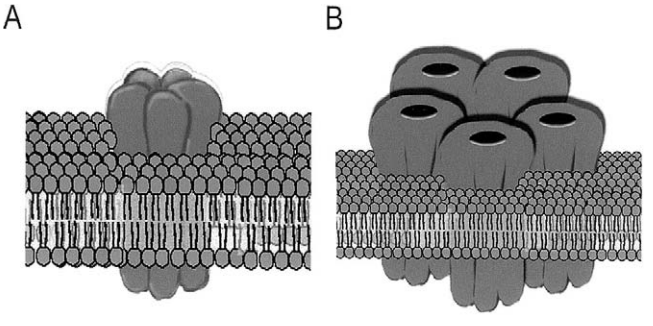


FIGURE 9 Illustration to indicate possible models that explain the substate behavior of GOLAC-2. (*A*) Single pore with five identical subunits. (*B*) Five identical pores that are physically linked, allowing them to enter a state in which they coordinately open or close.

second possibility is the ClC-0 channel from *Torpedo* electroplax, which is a two-barreled protein complex in which each pore can open independently or together in a coordinated fashion (Mindell et al., 2001; Weinreich and Jentsch, 2001). Additionally, it has been proposed that the large-conductance $Cl^-$ channel of alveolar epithelia is a co-channel complex containing six independent, but coordinately gated, conducting pathways (Krouse et al., 1986). The topic of co-channel behavior has been recently reviewed (Laver and Gage, 1997).

Our data favor the hypothesis that GOLAC-2 is a multipore co-channel complex because substate levels occurred in equal increments of ~65 pS, binomial analysis was consistent with each sublevel gating independently, and each open level had a similar mean dwell time of ~100 ms. Furthermore, each substate of GOLAC-2 behaved identically in all of the tests of single channel properties used (i.e., $E_{rev}$, $P_X/P_{Cl}$, $G_x/G_{Cl}$, block by DIDS and not IAA-94, pH-sensitivity, and activation by GSH). We propose that GOLAC-2 is a five-barreled co-channel (see Fig. 9 *B*) with pores that gate independently, but with an additional gate that can regulate the entire complex to produce full closings and openings.

Observations of GOLAC-2 kinetics showed that the channel fluctuates rapidly and randomly between open levels. We cannot rule out the possibility that the gating kinetics of GOLAC-2 are an artifact of the recording conditions in which regulatory peptides or molecules are lost in the fractionation procedure. Indeed, it would not be surprising if important regulatory mechanisms were missing in the artificial environment of the planar lipid bilayer. Potential physiological regulators of the Golgi anion channels need to be tested to obtain a clearer picture of their physiological roles. A recent review of chloride channels in hepatocytes, which is the tissue source for this study, points out the lack of a molecular identification for most of the general functions of anion channels (Li and Weinman, 2002). This disconnect between channels and their physiological relevance is especially acute for intracellular channels. Nevertheless, we speculate below on possible functions for GOLAC-2.

The observation that GOLAC-2 was not markedly pH sensitive in the physiological range does not exclude a role in maintaining charge balance of the Golgi complex. The conductance of GOLAC-2 is large and is probably more than sufficient to provide a source of $Cl^-$ ions to counter the charge translocated by the $H^+$ pump. GOLAC-2 was observed to have an inward rectification at potentials more negative than −75 mV that results from a larger (approximately twofold) single-channel current at negative membrane potentials. GOLAC-2 channels also showed a clear voltage-dependence of substate dwell times; the channel had longer dwell times at negative potentials for each of the open levels. Both the rectification and longer dwell times would be produced by a potential generated by the proton pump. These properties could help supply a constant source of $Cl^-$ anions for the Golgi lumen and are consistent with the proposed functional role of GOLAC-1 and -2 as a counter anion source for the organelle's $H^+$ pump. Additionally, a consequence of the constitutively open nature of GOLAC-2 (and GOLAC-1) may be to maintain a zero (or very small) membrane potential in the Golgi, which is essential for optimal activity of the $H^+$ pump (Glickman et al., 1983; Al-Awqati, 1995; Nordeen et al., 2000). An additional putative function for GOLAC-2 is to provide a pathway for organic anions, such as acetate, nitrate, sulfate, or inorganic phosphate to enter or exit the Golgi lumen. Anion exchange experiments demonstrated that the channel is permeable to many organic and inorganic species.

We have demonstrated that physiological levels of reduced GSH increase the conductance of GOLAC-2. This is an unusual effect on an ion channel and could arise from an allosteric effect caused by GSH binding or could be due to alterations in surface charge at the pore vestibule (Laver and Gage, 1997). What is the possible physiological significance of the GSH-sensitivity of GOLAC-2? Maintenance of cytoplasmic redox balance is achieved by the reduced (GSH) and oxidized (GSSG) forms of glutathione, which are found in millimolar concentrations in the cell. Consequently, glutathione is the major thiol-disulfide redox buffer of the cell. Glutathione is also a major buffer for free radicals, and its concentration will vary, for example during oxidative stress. Thus, GOLAC-2 is expected to be responsive to the redox state of the cell.

Does the Golgi need endogenous channels? In principle, itinerant ion channels and transporters that are in transit to other compartments or to the plasma membrane could set the ionic environment of the Golgi lumen. One problem with this scheme is that the Golgi would be subject to the vagaries of channel requirements and turnover in other cellular domains, rather than possessing its own regulation. A second problem with using transiting proteins to regulate the ionic composition of the Golgi is that many transiting proteins are not functional during their passage through the Golgi. For example, some proteins have "escort" proteins to keep them inactive until they reach their destination (Herrmann et al., 1999). For these reasons, we anticipated that the Golgi would have endogenous channels, and GOLAC-1 and 2 are the predominant channels we observe in the cyclohexamide-treated Golgi fraction. Do the two GOLACs share responsibilities, or in the extreme case, are they redundant? We have noted here that GOLAC-1 and GOLAC-2 have different biophysical properties, including pH sensitivity, suggesting that they have diverse functional roles. Thus, it seems more likely to us that GOLAC-1 and GOALC-2 have distinct sub-Golgi distributions, for example that one is in the *cis*- and the other in the *trans*-Golgi because each compartment carries out different functions.

We thank Dr. Diego Restrepo for providing the Levels software for mean-variance analysis and Dr. William Sather for critical reading of the manuscript. This work was supported by a grant from the National Insti-

tutes of Health, GM58987. R.J.T. is a recipient of a Natural Sciences and Engineering Research Council of Canada Postdoctoral Fellowship.

## REFERENCES


Al-Awqati, Q. 1995. Chloride channels of intracellular organelles. *Curr. Opin. Cell Biol.* 7:504–508.

Anderson, R. G., and R. K. Pathak. 1985. Vesicles and cisternae in the trans Golgi apparatus of human fibroblasts are acidic compartments. *Cell.* 40:635–643.

Berger, E. G., and J. Roth. 1997. The Golgi Apparatus. Birkhauser Verlag, Basel.

Berryman, M., and A. Bretscher. 2000. Identification of a novel member of the chloride intracellular channel gene family (CLIC5.) that associates with the actin cytoskeleton of placental microvilli. *Mol. Biol. Cell.* 11:1509–1521.

Bos, K., C. Wraight, and K. K. Stanley. 1993. TGN38 is maintained in the trans-Golgi network by a tyrosine-containing motif in the cytoplasmic domain. *EMBO J.* 12:2219–2228.

Bormann, J., O. P. Hamill, and B. Sakmann. 1987. Mechanism of anion permeation through channels gated by glycine and γ-aminobutyric acid in mouse cultured spinal neurones. *J. Physiol. (Lond.)* 385:243–286.

Clark, A. G., D. Murray, and R. H. Ashley. 1997. Single-channel properties of a rat brain endoplasmic reticulum anion channel. *Biophys. J.* 73: 168–178.

Colquhoun, D., and A. G. Hawkes. 1995. The principles of the stochastic interpretation of ion channel mechanisms. *In* Single Channel Recording. B Sakmann and E. Neher, editors. Plenum Press, New York. 397–482.

Colquhoun, D., and F. J. Sigworth. 1995. Fitting and statistical analysis of single-channel records. *In* Single Channel Recording. B Sakmann and E. Neher, editors. Plenum Press, New York. 483–587.

Dawson, D. C. 1996. Permeability and conductance of ion channels: a primer. *In* Molecular Biology of Membrane Transport Disorders. S. G. Schultz, T. E. Andreoli, A. M. Brown, D. M. Fambrough, J. F. Hoffman, and M. J. Welsh, editors. Plenum Press, New York. 87–110.

Demaurex, N., W. Furuya, S. D'Souza, J. S. Bonifacino, and S. Grinstein. 1998. Mechanism of acidification of the trans-Golgi network (TGN): in situ measurement of pH using retrieval of TGN38 and furin from the cell surface. *J. Biol. Chem.* 273:2044–2051.

Dulhunty, A., P. Gage, S. Curtis, G. Chelvanayagam, and P. Board. 2001. The glutathione transferase structural family includes a nuclear chloride channel and a ryanodine receptor calcium release channel modulator. *J. Biol. Chem.* 276:3319–3323.

Duncan, R. R., P. K. Westwood, A. Boyd, and R. H. Ashley. 1997. Rat brain p64H1, expression of a new member of the p64 chloride channel family in endoplasmic reticulum. *J. Biol. Chem.* 272:23880–23886.

Gaxiola, R. A., D. S. Yuan, R. D. Klausner, and G. R. Fink. 1998. The yeast CLC chloride channel functions in cation homeostasis. *Proc. Natl. Acad. Sci. U.S.A.* 95:4046–4050.

Glickman, J., K. Croen, S. Kelly, and Q. Al-Awqati. 1983. Golgi membranes contain an electrogenic $H^+$ pump in parallel to a chloride conductance. *J. Cell Biol.* 97:1303–1308.

Harrop, S. J., M. Z. DeMaere, W. D. Fairlie, T. Reztsova, S. M. Valenzuela, M. Mazzanti, R. Tonini, M. R. Qiu, L. Jankova, K. Warton, A. R. Bauskin, W. M. Wu, S. Pankhurst, T. J. Campbell, S. N. Breit, and P. M. G. Curmi. 2001. Crystal structure of the soluble form of the intracellular chloride channel ion channel CLIC1 (NCC27) at 1.4 A resolution. *J. Biol. Chem.* 276:44993–45000.

Herrmann, J. M., P. Malkus, and R. Schekman. 1999. Out of the ER: outfitters, escorts and guides. *Trends Cell Biol.* 9:5–7.

Hille, B. 2001. Ion Channels of Excitable Membranes, third edition, chapter 15. Sinauer Associates Inc., Sunderland, MA.

Hirschberg, C. B., P. W. Robbins, and C. Abeijon. 1998. Transporters of nucleotide sugars, ATP, and nucleotide sulfate in the endoplasmic reticulum and Golgi apparatus. *Ann. Rev. Biochem.* 67:49–69.

Jentsch, T. J., T. Friedrich, A. Schriever, and H. Yamada. 1999. The ClC chloride channel family. *Pflugers Arch. Eur. J. Physiol.* 437:783–795.

Kelly, R. B. 1985. Pathways of protein secretion in eukaryotes. *Science.* 230:25–32.

Kourie, J. I. 1998. Interaction of reactive oxygen species with ion transport mechanisms. *Am. J. Physiol.* 275:C1–C24.

Kourie, J. I., D. R. Laver, P. R. Junankar, P. W. Gage, and A. F. Dulhunty. 1996. Characteristics of two types of chloride channel in sarcoplasmic reticulum vesicles from rabbit skeletal muscle. *Biophys. J.* 70:202–221.

Krouse, M. E., G. T. Schneider, and P. W. Gage. 1986. A large anion-selective channel has seven conductance levels. *Nature.* 319:58–60.

Ladinsky, M. S., and K. E. Howell. 1992. The trans-Golgi network can be dissected structurally and functionally from the cisternae of the Golgi complex by brefeldin A. *Eur. J. Cell Biol.* 59:92–105.

Landry, D., S. Sullivan, M. Nicolaides, C. Redhead, A. Edelman, M. Field, Q. Al-Awqati, and J. Edwards. 1993. Molecular cloning and characterization of p64, a chloride channel protein from kidney microsomes. *J. Biol. Chem.* 268:14948–14955.

Laver, D. R., and P. W. Gage. 1997. Interpretation of substates in ion channels: unipores or multipores? *Prog. Biophys. Mol. Biol.* 67:99–140.

Li, X., and S. A. Weinman. 2002. Chloride channels and hepatocellular function: prospects for molecular identification. *Annu. Rev. Physiol.* 64:609–633.

Llopis, J., J. M. McCaffery, A. Miyawaki, M. G. Farquhar, and R. Y. Tsien. 1998. Measurement of cytosolic, mitochondrial and Golgi pH in single living cells with green fluorescent proteins. *Proc. Natl. Acad. Sci. U.S.A.* 95:6803–6808.

Mindell, J. A., M. Maduke, C. Miller, and N. Grigorieff. 2001. Projection structure of a ClC-type chloride channel at 6.5 A resolution. *Nature.* 409:219–223.

Morier, N., and R. Sauve. 1994. Analysis of a novel double-barreled anion channel from rat liver rough endoplasmic reticulum. *Biophys. J.* 67: 590–602.

Nagasawa, M., M. Kanzaki, Y. Iino, Y. Morishita, and I. Kojima. 2001. Identification of a novel chloride channel expressed in the endoplasmic reticulum, Golgi apparatus, and nucleus. *J. Biol. Chem.* 276: 20413–20418.

Nordeen, M. H., S. M. Jones, K. E. Howell, and J. H. Caldwell. 2000. GOLAC: an endogenous anion channel of the Golgi complex. *Biophys. J.* 78:2918–2928.

Patlak, J. B. 1993. Measuring kinetics of single ion channel data using mean-variance histograms. *Biophys. J.* 65:29–42.

Perez, M., and C. B. Hirschberg. 1987. Transport of sugar nucleotides into the lumen of vesicles derived from rat liver rough endoplasmic reticulum and Golgi apparatus. *Methods Enzymol.* 138:709–715.

Rousseau, E. 1989. Single chloride-selective channel from cardiac sarcoplasmic reticulum studied in planar lipid bilayers. *J. Membr. Biol.* 110:39–47.

Taylor, R. S., S. M. Jones, R. H. Dahl, M. H. Nordeen, and K. E. Howell. 1997. Characterization of the Golgi complex cleared of proteins in transit and examination of calcium uptake activities. *Mol. Biol. Cell.* 8:1911–1931.

Tulk, B. M., P. H. Schlesinger, S. A. Kapadia, and J. C. Edwards. 2000. CLIC-1 functions as a chloride channel when expressed and purified from bacteria. *J. Biol. Chem.* 275:26986–26993.

Varki, A. 1998. Factors controlling the glycosylation potential of the Golgi apparatus. *Trends Cell Biol.* 147:121–260.

van Meer, G. 2001. What sugar next? Dimerization of sphingolipid glycosyltransferases. *Proc. Natl. Acad. Sci. U.S.A.* 98:1321–1323.

Weinreich, F., and T. J. Jentsch. 2001. Pores formed by single subunits in mixed dimers of different ClC chloride channels. *J. Biol. Chem.* 276: 2347–2353.

Wright, E. M., and J. M. Diamond. 1977. Anion selectivity in biological systems. *Physiol. Rev.* 57:109–156.